Aligned deposition and electrical measurements on single DNA molecules

2015 Nanotechnology 26 475102

(http://iopscience.iop.org/0957-4484/26/47/475102)

IOP Publishing Nanotechnology
Nanotechnology 26 (2015) 475102 (8pp) doi:10.1088/0957-4484/26/47/475102

Aligned deposition and electrical measurements on single DNA molecules

Gennady Eidelshtein[1], Alexander Kotlyar[1], Mohtadin Hashemi[2,3] and Leonid Gurevich[2]

[1] Department of Biochemistry and Molecular Biology, George S Wise Faculty of Life Sciences and The Center of Nanoscience and Nanotechnology, Tel Aviv University, Ramat Aviv, Tel Aviv 69978, Israel
[2] Institute of Physics and Nanotechnology, Aalborg University, DK-9220 Aalborg East, Denmark
[3] Department of Pharmaceutical Sciences, University of Nebraska Medical Center, Omaha, NE 68198, USA

E-mail: s2shak@post.tau.ac.il and lg@nano.aau.dk

Received 26 June 2015, revised 19 September 2015
Accepted for publication 14 October 2015
Published 5 November 2015

Abstract

A reliable method of deposition of aligned individual dsDNA molecules on mica, silicon, and micro/nanofabricated circuits is presented. Complexes of biotinylated double stranded poly (dG)–poly(dC) DNA with avidin were prepared and deposited on mica and silicon surfaces in the absence of Mg^{2+} ions. Due to its positive charge, the avidin attached to one end of the DNA anchors the complex to negatively charged substrates. Subsequent drying with a directional gas flow yields DNA molecules perfectly aligned on the surface. In the avidin–DNA complex only the avidin moiety is strongly and irreversibly bound to the surface, while the DNA counterpart interacts with the substrates much more weakly and can be lifted from the surface and realigned in any direction. Using this technique, avidin–DNA complexes were deposited across platinum electrodes on a silicon substrate. Electrical measurements on the deposited DNA molecules revealed linear *IV*-characteristics and exponential dependence on relative humidity.

Keywords: avidin–DNA complex, directional deposition, AFM, electrical measurements

(Some figures may appear in colour only in the online journal)

1. Introduction

Ever since the discovery of the double-helix structure of DNA, researchers have strived to elucidate the relationships between its structural, chemical, and electrical properties. One of the most challenging issues has been the electrical conductivity of the molecule. The attempts to measure the electrical conductivity of DNA yielded very contradicting results, ranging from insulating [1, 2] to semiconducting [3] and even metallic behavior [4]. To a large extent, the origin of this controversy lies in the very nature of charge transport in DNA. The charge transport in DNA occurs through π–π stacking of the electronic orbitals of the neighboring bases and hence critically depends on their mutual orientation. As a result, while at short distances the coherent tunneling can be observed, at longer distances, due to structural defects and interaction with the environment, the molecule effectively breaks into segments between which thermally activated hopping occurs. This has recently been demonstrated experimentally for rigid and structurally uniform G4-DNA [5]. On the other hand, even for such rigid and uniform molecules, the extent of electron delocalization is limited to 10–11 tetrads. This observation shows the importance of a better understanding of the interaction between the DNA and the environment, and specifically finding ways to reduce structural distortions of soft and flexible DNA caused by its interaction with solid surfaces.

Typically, two main types of substrates are used for studies of DNA: mica plates and silicon wafers. Both of them exhibit negative surface charge at neutral pH. Because of that, adsorption of negatively charged molecules (DNA and proteins with pI lower then 7) on mica requires the presence of divalent metal ions, e.g. Mg^{2+}, Ni^{2+}, Mn^{2+}, and Co^{2+}. These cations serve as electrostatic bridges between the negatively charged DNA backbone and the mica surface enabling immobilization of the molecules (see, e.g. [6, 7]). Another approach, applicable to both mica and silicon oxide surfaces, involves covalent modification with aminosilane compounds

[8]. Positively charged amino groups introduced to the surface bind DNA molecules through electrostatic interactions with its backbone.

Deposition of DNA on hydrophobic surfaces has also been demonstrated. It involves partial unwinding of the DNA ends and interaction of nucleic bases of these unwound fragments with the surface by means of hydrophobic forces [9–11]. Although the latter approach enables alignment of molecules, strong interaction with the surface leads to deformation of the DNA and negatively affects its conducting properties (see, e.g. [12]).

Another critical issue related to conductivity of DNA molecules is humidity. Although it is well known that the structure of dsDNA critically depends on the level of its hydration (see, e.g. [13]), the effect of humidity on conductivity of the DNA is not well understood. It has been shown experimentally that an increase in relative humidity (RH) leads to an exponential increase in the DNA conductivity [14–16]. Recent theoretical studies by Bershevich and Chakraborty [17] have demonstrated that the hydration of DNA nucleobases leads to a significant narrowing of the band gap as well as the appearance of unbound π electrons and, as a result, significantly affects both electric and magnetic properties of DNA molecules.

In this study we demonstrate a new method of immobilization of DNA molecules on negatively charged mica and silicon surfaces in the absence of Mg^{2+}. The binding occurs through a positively charged avidin moiety attached to the biotinylated end of a long (thousands of base-pairs) poly (dG)–poly(dC) molecule. The immobilized molecules can be lifted from the surface and realigned. Using the above approach we positioned avidin–poly(dG)–poly(dC) complexes across nano-fabricated metal electrodes and measured their current–voltage (*IV*) characteristics.

2. Experiment

2.1. Materials and reagents

Unless otherwise stated, the reagents were obtained from Sigma-Aldrich (USA) and were used without further purification. Klenow fragment exonuclease minus of DNA polymerase I from *Escherichia coli* lacking the $3' \rightarrow 5'$ exonuclease activity (Klenow exo$^-$) was purchased from Thermo Scientific (USA).

2.2. DNA samples

The oligonucleotides were purchased from Alpha DNA (Montreal, Canada). In biotinylated $(dG)_{12}$-oligonucleotide (5′biotin–$(dG)_{12}$) the biotin residue is linked to the terminal base at the 5′-end. All oligonucleotides were purified by HPLC using Agilent 1100 HPLC system with a photodiode array detector. The $(dC)_{12}$-oligonucleotide were purified on an ion-exchange Western Analytical Products (USA) PolyWax LP column (4.6 × 200 mm, 5 μm, 300 Å). Oligonucleotides were eluted from the column in 10% acetonitrile with linear K-Pi (pH 7.5) gradient from 20 mM to 0.5 M for 1 h with flow rate of 0.8 ml min^{-1}. 5′biotin–$(dG)_{12}$ was purified using an ion-exchange HiTrap QHP column (5 × 1 ml) from GE Healthcare (USA) at pH 13. Elution was conducted in 0.1 M NaOH and 10% acetonitrile with a linear NaCl gradient from 0.5 to 1 M for 1 h at a flow rate of 0.7 ml min^{-1}. Peaks were identified by their retention times obtained from the absorbance at 260 nm. Purified oligonucleotides were desalted using pre-packed Sephadex G-25 DNA-Grade columns (Amersham-Biosciences). In order to create a double stranded template-primer, 5′biotin–$(dG)_{12}$–$(dC)_{12}$, $(dC)_{12}$ and 5′biotin–$(dG)_{12}$were incubated in 0.1 M NaOH at a molar ratio of 1:1 for 15 min and subsequently dialyzed against 20 mM Tris-acetate buffer, pH 7.5, for 4 h. All oligonucleotides were quantified spectrophotometrically using their respective extinction coefficients. The concentrations of 5′ biotin–$(dG)_{12}$and $(dC)_{12}$ oligonucleotides were calculated using extinction coefficients of 11.7 and 7.5 mM^{-1} cm^{-1} at 260 nm, respectively [18].

The DNA was synthesized according to the procedure described in our earlier work [19]. Briefly, the standard reaction contained 60 mM K-Pi, pH 7.4, 4 mM $MgCl_2$, 1 mg ml^{-1} BSA and 1.5 mM of dGTP and 1.5 mM dCTP, 0.2 μM Klenow exo$^-$ and 0.2 μM template-primer, 5′biotin–$(dG)_{12}$-$(dC)_{12}$. The reaction was performed at 8 °C for 14–16 h and triggered by the addition of the enzyme. The reaction was terminated by the addition of EDTA to a final concentration of 10 mM. The synthesized polymer, 5′biotin–poly(dG)–poly(dC) composed of 1000–2000 base pairs, was separated from the enzyme, NTPs, and other components of the assay on a Sepharose 2B column. The void volume fraction, containing 5′biotin–poly(dG)–poly(dC) was collected. The DNA concentration was estimated using molar extinction coefficient for GC pair of 14.8 mM^{-1}cm^{-1} at 260 nm [20].

5′biotin–poly(dG)–poly(dC) (60 nM in molecules) was incubated with strong molar excess of egg-white avidin (200 μM) in 0.2 M Tris base (pH ∼ 10.5) and 0.2 M NaCl for 1 h at 25 °C. The concentration of avidin was calculated using extinction coefficient of 97.4 mM^{-1} cm^{-1} at 280 nm [21]. The complex was separated from the excess of avidin on a Sepharose 2B column equilibrated with 0.2 M Tris base (pH ∼ 10.5) containing 0.2 M NaCl. The void volume fraction, containing 5′biotin–poly(dG)–poly(dC) was collected and stored at 4 °C. The purity of the avidin–5′biotin–poly (dG)–poly(dC) complex was confirmed by agarose gel electrophoresis.

2.3. Gel electrophoresis

The products of the polymerase synthesis were analyzed by 1% agarose gel electrophoresis at room temperature at 130 V for 1 h. TAE buffer was used for the agarose preparation and as a running buffer. The dimensions of the agarose gel were 10 × 10 cm with 2 × 4 mm 8-wells. The gel was stained with ethidium bromide (0.5 μg ml^{-1}) and visualized with a Bio Imaging System (302 nm).

2.4. AFM imaging

Atomic force microscopy was performed on the molecules adsorbed onto mica and silicon surfaces. 100 μl DNA solution (absorption was approximately 3 mOD at 260 nm) was used for the deposition. Samples were prepared using DNA in either 1 mM $MgCl_2$ or 20 mM LiCl in the case of Mg^{2+}-free deposition. Two types of substrates and incubation conditions were used: (1) freshly cleaved muscovite mica (Electron Microscopy Sciences, the USA), incubation for 5 min; (2) p-type silicon with 300 nm thermally grown oxide (NOVA Wafers, USA) with or without micro/nano fabricated electrodes, incubation for 10 min. Prior to incubation, the silicon substrates were cleaned using the standard RCA2 cleaning recipe (1:1:5 mixture of NH_4OH : H_2O_2 : H_2O at 70 °C). After incubation, the samples were rinsed with distilled water and dried with nitrogen gas. A nitrogen gun was tilted to roughly 45° with respect to either mica or silicon substrate and kept in the same direction until the substrate was completely dry. Otherwise, no other special precautions were taken; centralized laboratory nitrogen supply (5 bar) was used in the experiments. No dissociation of biotin from avidin was observed at the nitrogen flow rates used. The same rinsing/drying procedure was used for both Mg^{2+}- and avidin-assisted deposition.

AFM images were obtained with a Solver PRO (NT-MDT, Russia) and NTegra Aura (NT-MDT, Russia) AFMs in the intermittent-contact (tapping) mode using Si-cantilevers (NT-MDT, Russia and Olympus, Japan) with resonance frequency of 90–150 kHz. The images were 'flattened' (each line of the image was fitted to a 2nd-order polynomial, and the polynomial was then subtracted from the image line) using the AFM image-processing software. The images were analyzed and visualized using a Nanotec Electronica S.L (Madrid) WSxM [22] and Gwyddion [23] image-processing software.

2.5. Electron-beam lithography

The electrodes were produced using a two-step lithographic process involving optical and electron beam lithography. First, a coarse pattern was fabricated on 4″ Si-wafers with 300 nm thermally grown oxide using optical lithography followed by thermal evaporation of 5 nm of Cr and 70 nm of Au in a Cryofox Explorer 600 (Polyteknik A/S) and subsequent lift-off. After verification of the pattern, the silicon wafer was diced into 10 × 10 mm substrates containing one coarse electrode pattern each.

For electron-beam lithography, the 10 × 10 mm substrates were coated with a 200 nm layer of 1.5% 950k PMMA (MicroChem) in chlorobenzene and the fine pattern was written using an Elphy Plus (Raith Nanofabrication, Germany) installed on a 1540XB Cross-Beam SEM (Zeiss, Germany). After development in cold 3:1 (v/v) IPA: methyl isobutyl ketone with 1.5 vol% methyl ethyl ketone [24], substrates were subjected to thermal evaporation of 1 nm Cr and 5 nm Pt and lift-off. Finally, the electrodes were cleaned in RCA2 solution and the obtained patterns were inspected by SEM and AFM. The produced interdigitated electrodes had a typical width and inter-electrode spacing of 50 nm.

2.6. Electrical measurements

Deposition technique described above was used to deposit avidin–DNA complexes on electrode substrates in such a way that they cross two or more electrodes. Unless otherwise stated, after deposition of DNA, the samples were dried in vacuum for 30 min and subsequently inspected with AFM. If indicated, hydration of the sample was done by placing 100 uL H_2O on the surface for 15 s followed by drying with nitrogen gas. The *IV* characteristics were acquired using a PM5 probe station (SÜSS MicroTec) connected to a Model 6517A source-electrometer (Keithley Instruments) in a two-point geometry. The probe station was placed in a sealed Faraday cage, which was also used to create a controlled environment. Humidity inside the probe station was controlled by the flow of humidified compressed air. RH was measured continuously using a digital hygrometer 485 series (Dwyer Instrument, USA). Prior to the measurements, the humidity was stabilized for at least one minute and then continuously maintained during the measurements.

The measurements were controlled by custom software written in LabVIEW (National Instruments). Briefly, the software allowed sweeping voltage across the electrodes with a given rate while monitoring the current flowing between them. A typical experiment involved one or several sweeps in the range of ±5 V with a scan rate of 30 mV s^{-1}. The typical noise level was below 150 fA rms. During all stages of the measurement, two 1 MOhm resistors were connected in series to the electrodes to prevent damage of DNA by excessive current (e.g. due to an electrostatic discharge). Other standard measures against electrostatic discharge were implemented as well.

3. Results and discussion

We have shown (see figure 1) that avidin–DNA complexes efficiently bind to a mica surface in the absence of Mg^{2+} ions, in contrast to DNA molecules which can be deposited only in the presence of the cation. The molecules deposited in the absence of Mg^{2+} appear to be well aligned on the surface (see figure 1(A)), in contrast to those immobilized in the presence of the cation (figure 1(B)). In the latter case the molecules are randomly positioned on the surface.

The direction of DNA molecules on the surface is governed by the direction of gas flow during the drying procedure. A schematic illustration of the deposition method is shown in figure 2. The first step involves electrostatic binding of a positively charged avidin moiety of an avidin–DNA complex to negatively charged mica (figure 2(A)). The negatively charged DNA backbone cannot bind to the surface due to the electrostatic repulsion, hence preventing the DNA molecules from irreversible adsorption on mica. In other words, the DNA molecule does not reach the primary minimum of the DLVO forces and remains in the secondary

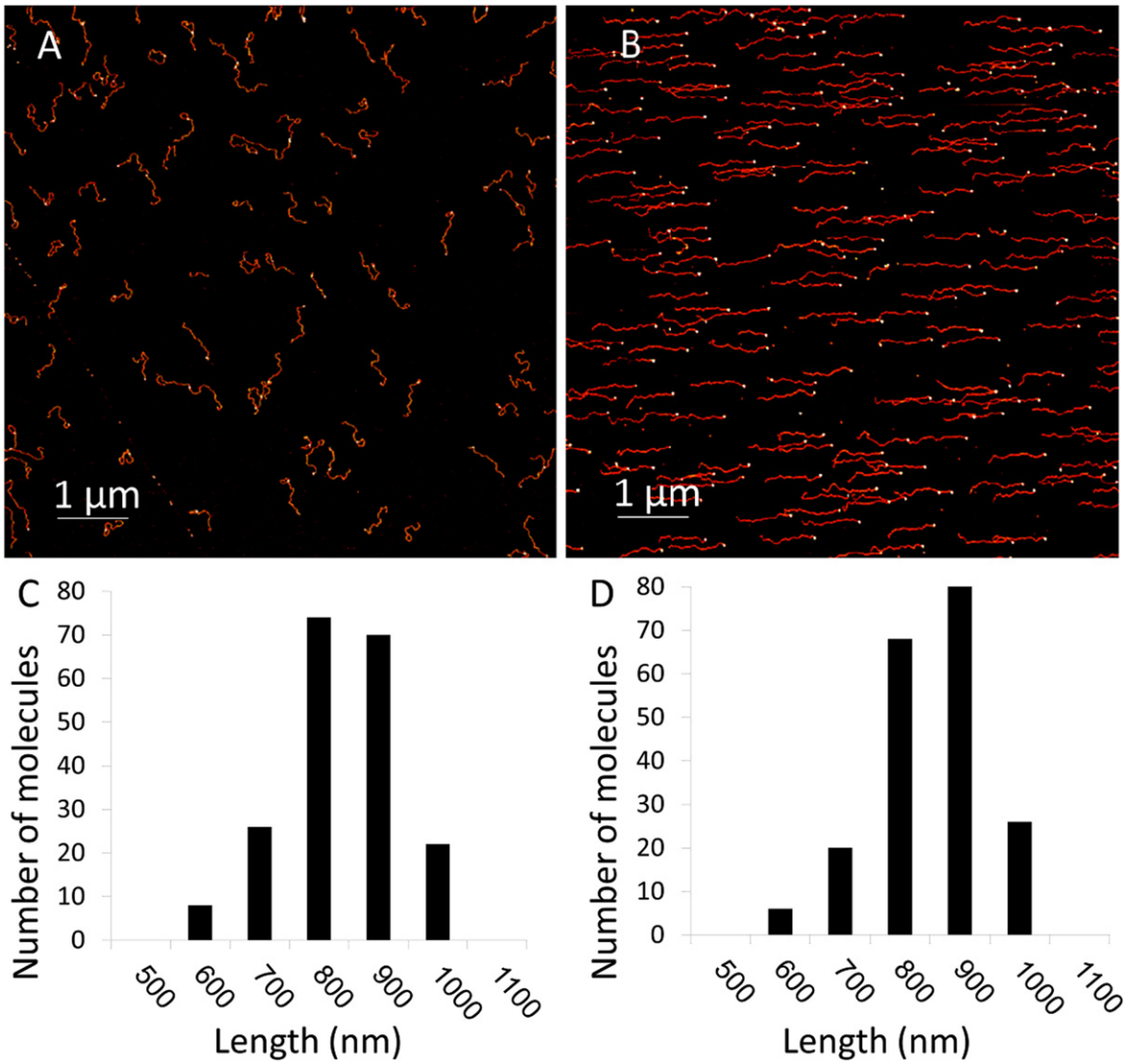

Figure 1. Deposition of avidin–DNA on mica in the presence (A) and the absence (B) of magnesium ions. (A) Deposition was carried out in 1 mM Mg-acetate for 5 min. (B) Deposition was in 20 mM LiCl for 5 min. The surface was rinsed with double distilled water and dried with N_2. (C) and (D) show statistical contour length analysis of approximately 200 molecules in (A) and (B) respectively. Tip convolution is taken into account by subtracting the tip diameter from the measured length.

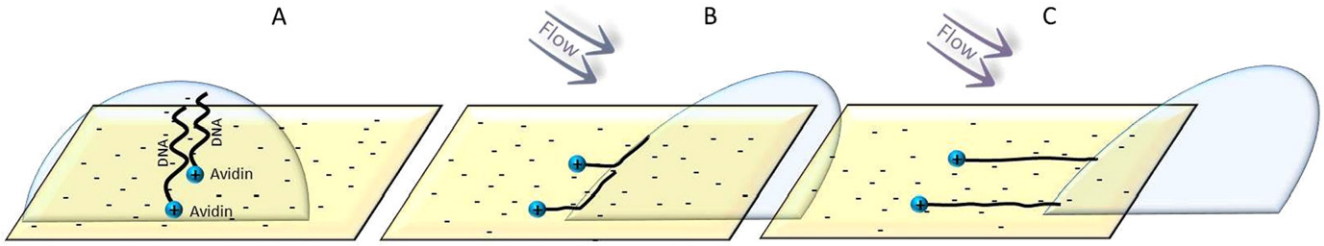

Figure 2. A tentative scheme for avidin–DNA deposition on mica. (A) Binding of positively charged avidin moieties (blue spheres) to a negatively charged surface by means of electrostatic forces. (B) Initial stage of the surface drying with nitrogen gas. A drop of water is partly removed from the surface. DNA (black lines) is forced to approach the surface. (C) A drop of water is completely removed. DNA molecules are aligned on the surface in the direction of the gas flow.

minimum, where the attractive van der Waals interactions are balanced by the repulsive electrostatic forces. Immobilization of the DNA takes place only upon drying the surface with nitrogen gas. It should be noted that although this technique involves alignment of DNA by meniscus forces, similar to various combing techniques [11], the average contour length of the molecules deposited by the technique described here is equal, within the experimental error, to that of the molecules

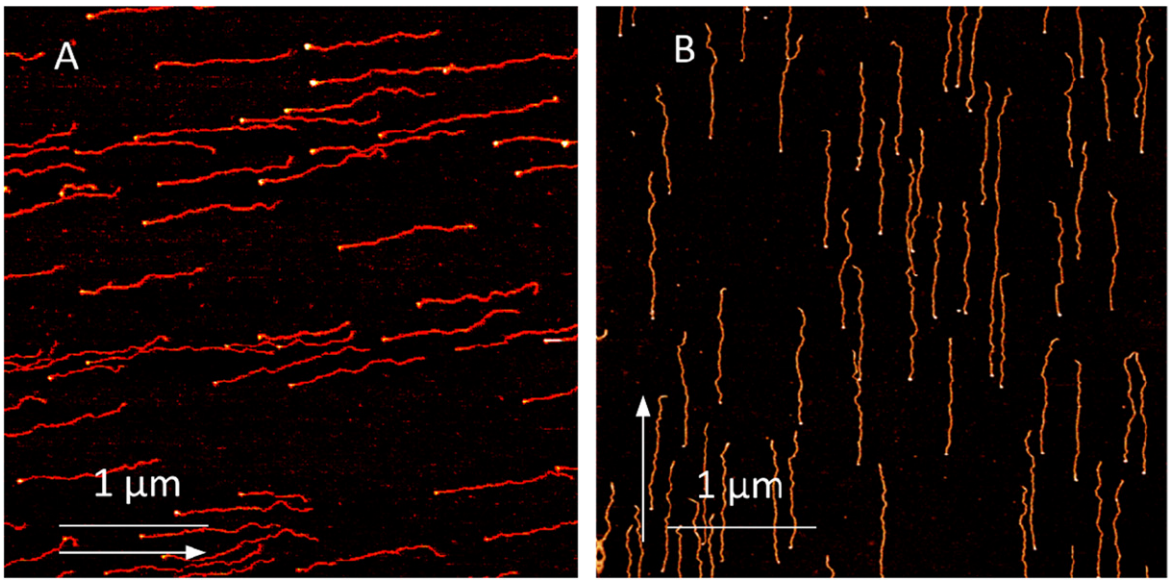

Figure 3. Reorientation of avidin–DNA complexes on a mica surface. (A) The molecules were adsorbed on mica in 20 mM LiCl as in figure 1(B) and dried by nitrogen gas. The direction of the nitrogen flow is indicated by the arrow. (B) A drop (50 μl) of double distilled water was placed on the surface (imaged in A) and incubated for 5 min. The surface was then dried by nitrogen gas in the direction (indicated by the arrow) perpendicular to the initial one.

deposited using classical magnesium-mediated adsorption technique (see panels C and D in figure 1). This can be contrasted to a considerable (up to 160%) overstretching of DNA commonly observed during combing. We believe that this difference is attributed to a much weaker interaction of DNA molecules with the surface in our case as compared to previously reported combing techniques.

Moreover, the DNA molecules deposited using our technique can be detached from the surface while the avidin moiety remains electrostatically pinned to the surface. Then, it is possible by pouring a drop of water or buffer on the surface to lift the molecules and re-adsorb them while drying. This is in contrast to DNA molecules deposited in the presence of Mg^{2+}, which always remain tightly bound to the surface. As seen in figures 3(A) and (B), adding a droplet of water to a mica surface with aligned avidin–DNA complexes and subsequently drying, with a nitrogen stream in a direction perpendicular to that used for the deposition, yields molecules aligned perpendicular to the initial direction. This shows that DNA molecules can be lifted and subsequently realigned on the surface. On the other hand, the molecules deposited in the presence of Mg^{2+} are very tightly bound to the surface and cannot be repositioned (data not presented). These results suggest that the structure and properties of the molecules deposited by our techniques are less affected by interaction with the surface as compared to those deposited in the presence of Mg^{2+} ions.

Direct measurements of electrical transport through single DNA molecules are very challenging and require controlled deposition of molecules across the electrodes. The fabrication of electrodes for electrical measurements is commonly performed on a silicon substrate. In order to attract DNA molecules to the silicon substrate, positively charged residues (commonly, amino groups) are introduced to the surface. Deposition of DNA on the aminosilane-modified wafer is typically directionless, leading to a very low yield of molecules crossing the electrodes. Moreover strong electrostatic attraction of the DNA molecule bridging the electrodes to the positively charged aminosilane-modified silicon surface might strongly affect the conformation of the double helix 'bridge' and as a result, significantly hinder the ability of the DNA molecule to conduct electrical current. As shown in figure 4(A), the use of the avidin–DNA complex makes it possible to adsorb DNA on a bare silicon surface. As in the case of mica, the avidin-anchored molecules are aligned on the Si surface along the direction of the gas stream. Blowing the gas in the direction perpendicular to the electrodes results in molecules crossing the electrodes (see figure 4(B)). It is important to emphasize that the molecules positioned across the electrodes experience repulsion from the negatively charged substrate. The repulsive forces prevent them from bending at the electrode edge and sagging onto the silicon surface. The structure and properties of DNA molecules are therefore less affected by the surface as compared to those deposited on an aminosilane-modified silicon.

It is known that the conductivity of DNA in general and poly(dG)–poly(dC) in particular strongly depends on RH [14]. The electrical measurements were conducted on several different nanoelectrode substrates, typically containing 2–4 poly(dG)–poly(dC) molecules bridging the electrodes. While freshly deposited samples exhibited linear hysteresis-free *IV*-characteristics, exposure to a dry atmosphere considerably reduced the current. Initial conductivity could be restored by rehydration of the sample as described in Experimental section. The molecules could be subjected to several (three and more) drying-rehydration cycles without a noticeable

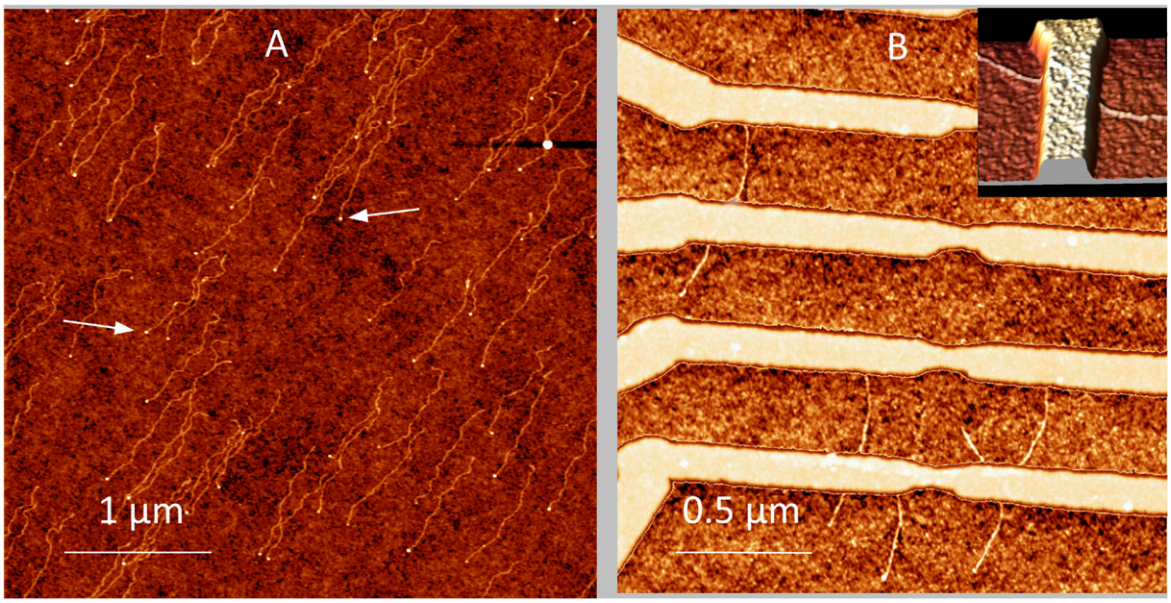

Figure 4. Deposition of avidin–DNA molecules on a bare silicon surface and across the nanofabricated platinum electrodes (approximately 7 nm high). An avidin–DNA complex was prepared as described in materials and methods. The avidin–DNA solution in 20 mM LiCl was placed on a silicon wafer and incubated for 5 min. The sample was then rinsed with double distilled water and dried with nitrogen gas: (A)—a region of bare silicon surface away (∼1 mm) from the electrode's avidin heads is indicated by the arrows; (B)—the electrode region. The inset shows a 3D zoom image of the DNA molecule crossing the electrode (color balance is locally changed).

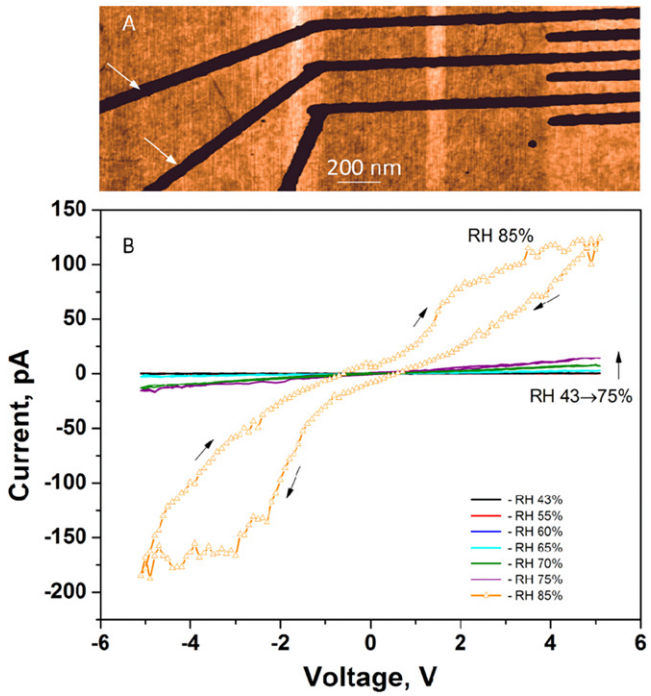

Figure 5. Electrical measurements on avidin–DNA complexes deposited on Pt electrodes. (A)—AFM image of electrodes (indicated by the arrows) with DNA molecules deposited across them (dark lines). (B)—*IV*-characteristic obtained at different (from 43% to 85%) values of relative humidity. The *IV*-characteristics were obtained at a scan rate of approximately 30 mV s^{-1} at 21 °C.

change in their *IV* characteristics. Despite some variation in conductivity of different samples with a similar number of bridging DNA molecules measured under identical experimental conditions, which we attribute to variations in the contact resistance (also observed e.g. in [5]), an increase in the number of DNA molecules bridging the electrodes always led to an increase in the conductivity.

One of the samples, shown in figure 5(A) (DNA molecules are shown as dark lines) was selected to perform detailed measurements at different values of RH (figure 5(B)). The measurements at ambient humidity (set to 43% in the clean room environment) exhibited no current above the noise level (∼150 fA) for a ±5 V sweep. Increasing humidity above 55% RH led to linear hysteresis-free *IV*-characteristics. This tendency continued up to approximately 75%–80% RH, above which a significant non-linearity and hysteresis was observed (figure 5). These data obtained at high RH resembled a cyclic voltammogram, hence indicating an onset of electrochemical reaction on a chip. On the other hand, in the humidity range from 43% to 75% a clear exponential dependence of the resistance on RH was found (see figure 6).

It is interesting to compare the results presented in figure 6 with the data obtained earlier [14] on the DNA molecules of the same sequence. In contrast to our experiments conducted on a small (2–4) number of poly(dG)–poly(dC) molecules, in the cited work an unspecified large number of the molecules was deposited on top of nanofabricated electrodes and subjected to electrical measurements. It has been shown that while two-probe measurements exhibit

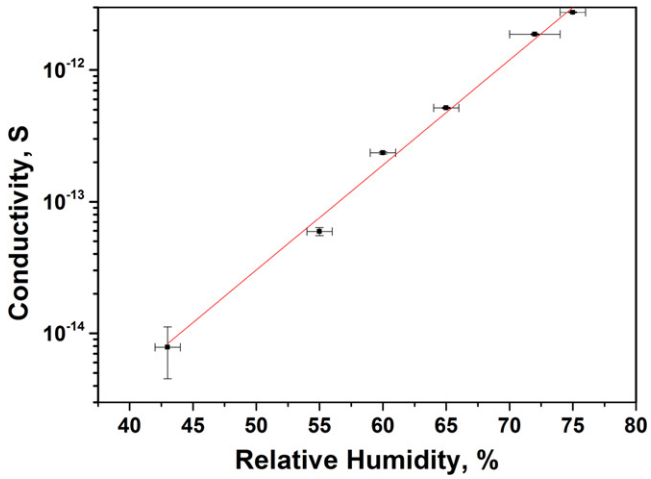

Figure 6. The dependence of the DNA conductivity on RH.

highly non-linear hysteretic behavior with a gap-like feature, four-point measurements (i.e. with the contact resistance excluded) show linear and hysteresis-free behavior. In our case, two-point measurements demonstrated essentially linear behavior with minor or even no hysteresis, indicating a reduced contact resistance at the DNA–electrode interface. We attribute this difference to lower deformations of DNA molecules induced by interaction with electrodes. The DNA hydration restores the native structure of DNA and leads to a thousand-fold increase in conductivity upon increasing the humidity, well in line with the theoretical predictions [17]. Further increase in RH leads to formation of a continuous water layer along the DNA molecule and an onset of electrochemical processes. It should be noted that the significantly cleaner silicon surfaces and the use of low concentration of synthetic DNA, as compared to the high concentration of the genomic DNA in [16], allowed us to separate the 'intrinsic' DNA properties and the onset of water hydrolysis.

4. Conclusion

In summary, we developed a new DNA deposition technique suitable for aligned deposition of single DNA molecules on negatively charged surfaces, e.g. mica and silicon oxide. This technique significantly reduces DNA interaction with the surface and allows lifting the molecules and repositioning them on the surface. We employed this technique for electrical characterization of single poly(dG)–poly(dC) DNA molecules deposited across nano-fabricated electrodes. We demonstrated that the DNA molecules exhibit essentially linear and hysteresis-free *IV*-characteristics in the range of RH from 43% to 75%. Moreover, in line with the published data, the conductance of tested molecules showed exponential dependence on RH. At higher values of RH, a hysteretic non-linear behavior was observed indicating an onset of electrochemical reactions in the water layer surrounding the molecule.

Acknowledgments

The authors acknowledge Velux Visiting Professor Programme that has greatly supported discussion and experimental work leading to this application. We are also grateful to The Obel Family Foundation for the financial support and to the Israel Science Foundation (grant 172/10).

References

[1] de Pablo P J, Moreno-Herrero F, Colchero J, Gomez Herrero J, Herrero P, Baro A M, Ordejon P, Soler J M and Artacho E 2000 Absence of dc-conductivity in lambda-DNA *Phys. Rev. Lett.* **85** 4992–5

[2] Storm A, Van Noort J, De Vries S and Dekker C 2001 Insulating behavior for DNA molecules between nanoelectrodes at the 100 nm length scale *Appl. Phys. Lett.* **79** 3881–3

[3] Porath D, Bezryadin A, De Vries S and Dekker C 2000 Direct measurement of electrical transport through DNA molecules *Nature* **403** 635–8

[4] Kasumov A Y, Kociak M, Gueron S, Reulet B, Volkov V, Klinov D and Bouchiat H 2001 Proximity-induced superconductivity in DNA *Science* **291** 280–2

[5] Livshits G I *et al* 2014 Long-range charge transport in single G-quadruplex DNA molecules *Nat. Nanotechnology* **9** 1040–6

[6] Brack C and Griffith J D 1981 DNA electron microscopy: I *Crit. Rev. Biochem. Mol. Biol.* **10** 142–69

[7] Hansma H, Vesenka J, Siegerist C, Kelderman G, Morrett H, Sinsheimer R, Elings V, Bustamante C and Hansma P 1992 Reproducible imaging and dissection of plasmid DNA under liquid with the atomic force microscope *Science* **256** 1180–4

[8] Shlyakhtenko L S, Gall A A, Filonov A, Cerovac Z, Lushnikov A and Lyubchenko Y L 2003 Silatrane-based surface chemistry for immobilization of DNA, protein–DNA complexes and other biological materials *Ultramicroscopy* **97** 279–87

[9] Klein D, Gurevich L, Janssen J, Kouwenhoven L, Carbeck J and Sohn L 2001 Ordered stretching of single molecules of deoxyribose nucleic acid between microfabricated polystyrene lines *Appl. Phys. Lett.* **78** 2396–8

[10] Nazari Z E and Gurevich L 2013 Controlled deposition and combing of DNA across lithographically defined patterns on silicon *Beilstein J. Nanotechnol.* **4** 72–6

[11] Nazari Z E and Gurevich L 2013 Molecular combing of DNA: methods and applications *J. Self-Assem. Mol. Electron.* (*SAME*) **1** 125–48

[12] Gutiérrez R, Porath D and Cuniberti G 2006 DNA conduction: the issue of static disorder, dynamic fluctuations and environmental effects *Charge Transport in Disordered Solids with Application in Electronics* ed S Baranovski (Chichester: Wiley) ch 12

[13] Bates A D and Maxwell A 2005 *DNA Topology* (New York: Oxford University Press)

[14] Ha D H, Nham H, Yoo K-H, So H-M, Lee H-Y and Kawai T 2002 Humidity effects on the conductance of the assembly of DNA molecules *Chem. Phys. Lett.* **355** 405–9

[15] Tuukkanen S, Kuzyk A, Toppari J J, Hytönen V P, Ihalainen T and Törmä P 2005 Dielectrophoresis of nanoscale double-stranded DNA and humidity effects on its electrical conductivity *Appl. Phys. Lett.* **87** 183102

[16] Kleine-Ostmann T, Jördens C, Baaske K, Weimann T, de Angelis M H and Koch M 2006 Conductivity of single-stranded and double-stranded deoxyribose nucleic acid

under ambient conditions: the dominance of water *Appl. Phys. Lett.* **88** 102102
[17] Berashevich J and Chakraborty T 2008 How the surrounding water changes the electronic and magnetic properties of DNA *J. Phys. Chem.* B **112** 14083
[18] Cantor C R, Warshaw M M and Shapiro H 1970 Oligonucleotide interactions: III. Circular dichroism studies of the conformation of deoxyoligonucleolides *Biopolymers* **9** 1059–77
[19] Kotlyar A B, Borovok N, Molotsky T, Fadeev L and Gozin M 2005 *In vitro* synthesis of uniform poly (dG)–poly (dC) by Klenow exo-fragment of polymerase I *Nucleic Acids Res.* **33** 525–35
[20] Inman R and Baldwin R 1964 Helix-random coil transitions in DNA homopolymer pairs *J. Mol. Biol.* **8** 452–69
[21] Inoue H, Sato K and Anzai J-I 2005 Disintegration of layer-by-layer assemblies composed of 2-iminobiotin-labeled poly(ethyleneimine) and avidin *Biomacromolecules* **6** 27–9
[22] Horcas I, Fernández R, Gómez-Rodríguez J M, Colchero J, Gómez-Herrero J and Baro A M 2007 WSXM: a software for scanning probe microscopy and a tool for nanotechnology *Rev. Sci. Instrum.* **78** 013705
[23] Nečas D and Klapetek P 2012 Gwyddion: an open-source software for SPM data analysis *Cent. Eur. J. Phys.* **10** 181–8
[24] Hu W, Sarveswaran K, Lieberman M and Bernstein G H 2004 Sub-10 nm electron beam lithography using cold development of poly(methylmethacrylate) *J. Vac. Sci. Technol.* B **22** 1711